A Wireless Battery-Free Cerebral-Oxygen-Monitoring Micro-System Featuring 0.028% Sensing Resolution

Weixiao Wang, Boyu Zhu, Yangfan Xuan, Yili Shen, Qijing Xiao, Zhiyu Wang, Yuxuan Luo, Gang Pan, Bin Su, Bo Zhao

Zhejiang University, Hangzhou, China

Cerebral oxygen monitoring (COM) presents the partial pressure of oxygen (PO_2) in human brain, which helps with the treatment of various brain diseases such as traumatic brain injury (TBI). Long-termly COM can detect the potential cerebral hypoxia due to severe brain injuries, which is necessary in invasive medical treatment for TBI patients. To conduct accurate portable diagnosis in a long term, the COM devices are required to be wireless, high-resolution, long-lifetime, and miniature. Traditional PO_2 sensing products such as Licox relied on bulk hardware and cables, which was not suitable for long-term portable monitoring. In recent years, plenty of researches try to change the bulky cable-based COM instruments into portable wireless devices, where low-power techniques are studied to extend the lifetime. As shown in Fig.1, there are two conventional PO_2 sensing methods: 1) Optical sensing method. A 4.5mm^3 optical PO_2 sensing device offered a resolution up to 0.09% [1], but the power-hungry LED driver limited the life time. For example, the LED driver consumed 20mW power in [3], which presented to be the bottleneck in long-termly monitoring. 2) Electrochemical sensing. A resolution of ±0.13% was achieved by a 42μW cable-based electrochemical sensor [2]. Then, the PO_2 sensing resolution was improved to 0.06% in [5], while it's at the penalty of 1.4mW power consumption due to the power-hungry trans-impedance amplifier (TIA). As a result, it's difficult for the conventional COM devices to realize both a high resolution and a low power.

To address the issues in conventional COM devices, we demonstrate a wireless battery-free COM micro-system: 1) A sensing-current-reuse technique is proposed to break down the system power to 25μW, which enables battery-free wireless telemetry through a 2m range. 2) A bipolar residual zoom-in (BRZ) technique is proposed to improve the sensing resolution to 0.028%. In this way, the proposed techniques offer a portable high-precision device for long-term COM applications.

The top-level block diagram of the COM micro-system is depicted in Fig.2. The system consists of an antenna, a power-supply module, a potentiostat with a sensing current detector, and a telemetry module. The antenna and power-supply module harvest RF energy from a 434MHz router, and provide DC power for all the submodules. The potentiostat biases the three electrochemical electrodes, i.e., working electrode (WE), reference electrode (RE), and counter electrode (CE), to extract the sensing current of cerebral oxygen. The sensing current is then converted into a digital bitstream by two-step quantization based on the proposed BRZ technique, to achieve a high sensing resolution. To cut down the power consumption for battery-free operation, the sensing current is reused to power the sensing current detector, which also eliminates the power-hungry TIA and current mirror in conventional current-detection structures. Finally, the data of sensing current are backscattered to the router as the wireless telemetry.

In conventional potentiostat of electrochemical sensor-interface chip, the power budge is dominated by the OTAs, current mirror, and data converter. As shown in Fig.3(top-left), the multiple OTAs set the biasing voltage between WE and RE, and the current mirror extracts the sensing current. The OTAs should be designed with a high gain to provide sufficient precision and linearity of the PO_2 sensor. To realize a sufficient resolution, the secondary current of current mirror should be equal or larger than the primary current. In addition, an ADC is required to convert the current signal into digital bits for wireless telemetry. As a result, considerable power is dissipated by the OTAs, current mirror, and ADC in the electrochemical sensing system.

A sensing-current-reuse technique is proposed to reduce the power consumption. As illustrated in Fig.3(top-right), the sensing current I_{SENS} is reused to power the subsequent data converters, saving the power consumption in current detecting. Meanwhile, I_{SENS} is directly converted into digital bits without a current mirror. Moreover, the proposed circuit only needs a single OTA, while the WE is intermittently switched to an ultra-low-power buffer to calibrate the WE potential voltage V_{WE}. In this way, the total power consumption of electrochemical sensing can be significantly reduced, realizing a sensing-current-reused TIA-less current-mirror-less potentiostat. The sensing current detector inside, given in Fig. 3(bottom-left), consists of a dynamic comparator, a SAR current digital-to-analog convertor (IDAC), a BRZ IDAC, digital logic, and an integration capacitor. I_{SENS} charges the integration capacitor C_{INT} , which is discharged by I_{DAC}, the current generated by IDACs. The overall target of the logic is to automatically tune the I_{DAC} to be equal to I_{SENS}, resulting in a stable potential voltage on C_{INT} as V_{WE}. Meanwhile, the control bits of IDACs reflect the magnitude of I_{SENS}, which will be sent to a remote router through far-field backscattering communication.

The BRZ technique is proposed to improve the resolution in the sensing-current-reused potentiostat. The timing waveforms are given in Fig.3(bottom-right), where the proposed BRZ technique further quantizes the residual current $I_{RES} = I_{SENS} - I_{SAR}$ after I_{SENS} resolved by the SAR logic, improving the sensing resolution. During the SAR phase, V_{WE} is first settled by the buffer to re-establish the preset reference voltage $V_{WE,REF}$. Then, the WE is switched to the SAR IDAC in the sensing current detector, where I_{SENS} and the SAR IDAC current I_{SAR} charges/discharges the integration capacitor C_{INT} . With the SAR logic, I_{SAR} approaches I_{SENS} rapidly. The BRZ logic judges the polarity of residual current I_{RES} by comparing V_{WE} with $V_{WE,REF}$. According to the polarity, the BRZ logic controls the on/off states of the BRZ IDAC by Φ_1 or Φ_2 to further adjust I_{DAC}, resulting in a V_{WE} voltage fluctuating around $V_{WE,REF}$. Meanwhile, I_{RES} is zoomed in and digitized. During the BRZ phase, the BRZ IDAC current I_{BRZ} and the residual current I_{RES} induce the same amount of charge on the integration capacitor. Thus, I_{RES} can be derived as:

$$I_{RES} = I_{BRZ} \cdot N_{\Phi_1,\Phi_2} / N_{TOTAL}, \quad (1)$$

where $N_{\Phi1,\Phi2}$ stands for the clock cycles for the on state of BRZ IDAC, and N_{TOTAL} represents the total clock cycles in BRZ Logic phase except for the I_{RES} polarity judging period. Due to the bipolar judgement, the BRZ technique covers a wider range of residual current left by the SAR IDAC.

Figure 4(top-left) details the 3D structure and scanning electron microscopy images of WE fabricated on a piece of carbon fiber electrode (CFE). Figure 4(top-right) gives the structure of proposed antenna and its simulated radiation pattern. The performance of current sensing is measured in Fig.4(bottom). The chip detects the maximal sensing current of 1uA with a linearity of R^2=0.9993. At a constant input of 200nA, 500 samples of sensing current are measured, where the standard deviation is less than 129pA (1σ), indicating a dynamic range of 77.8dB. The *in-vitro* measurement setup is shown in Fig.5(left). Artificial cerebrospinal fluid (ACSF) is used to mimic the cerebral environment. The time-domain backscatter waveform is captured in Fig.5(top-right) and the detected sensing currents averaged in 20 consecutive samples is depicted in Fig.5(bottom-right). The specific PO_2 values are marked on the currents, where the proposed BRZ technique enables the micro-system to achieve a PO_2 sensing resolution up to 0.028%. The performance of wireless power transfer in battery-free operation is measured, to illustrate the required power emitted by the router versus the power-transfer range, as shown in Fig.6(top-left).

Figure 6(top-right) shows the power breakdown of the proposed COM micro-system, and Fig.6(bottom) summarizes the measurement performance and compares with the state of the arts. The comparison shows that: 1) The proposed COM micro-system achieves the best resolution among all the works, benefiting from the proposed BRZ technique. 2) The proposed sensing-current-reuse technique reduces the power consumption to be lowest among all the chips, enabling 2m-range battery-free readout. Fabricated in 55nm CMOS process, the chip takes a total area of 0.93mmx0.61mm including I/O frame and the die micrograph is illustrated in Fig.7.

This work was supported by the National Key R&D Program of China under Grant 2023YFF1203600. Corresponding Author: Bo Zhao (zhaobo@zju.edu.cn).

References:

[1] S. Sonmezoglu *et al.*, "A 4.5mm^3 deep-tissue ultrasonic implantable luminescence oxygen sensor," ISSCC, 2020

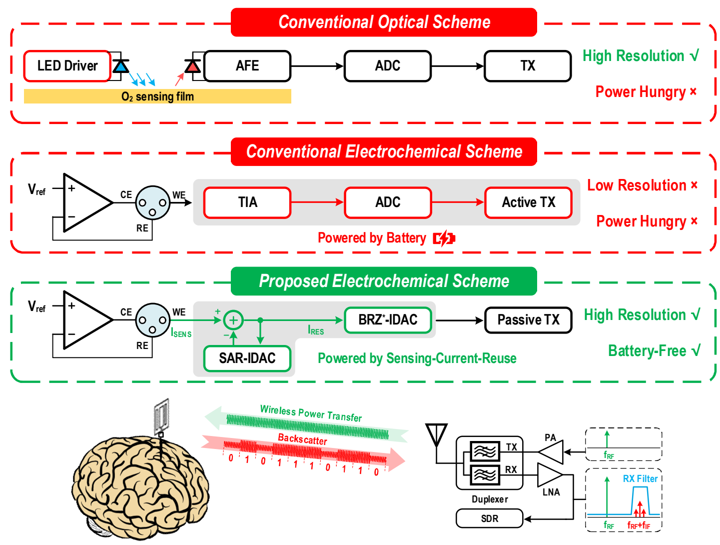

Fig. 1 Conventional PO_2 sensing techniques and proposed wireless battery-free cerebral oxygen monitoring (COM) micro-system.

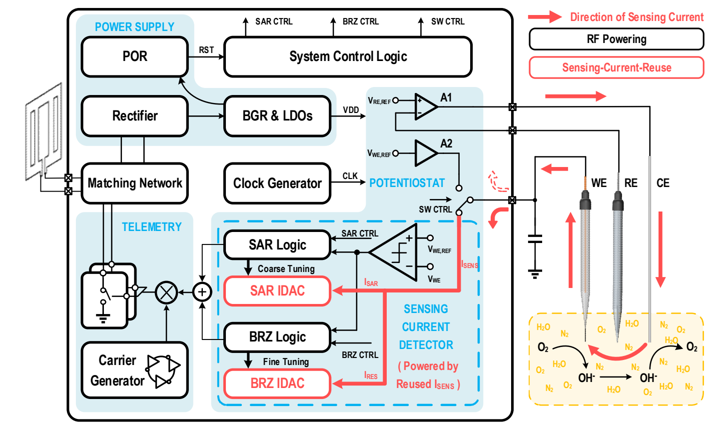

Fig. 2 Top-level block diagram of proposed cerebral oxygen monitoring (COM) micro-system and concept of electrochemical PO_2 sensing.

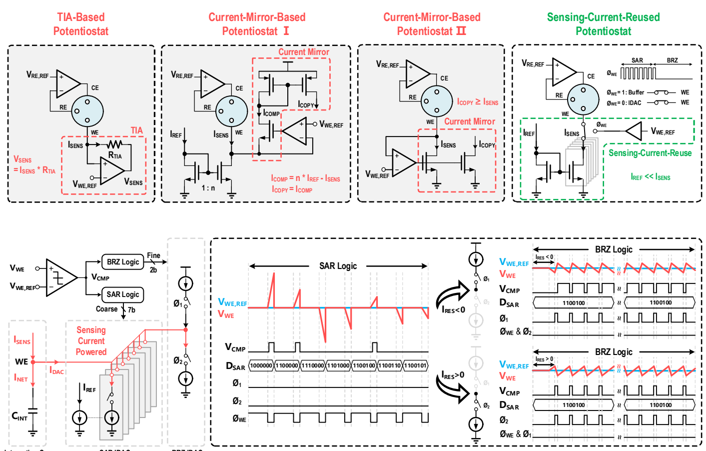

Fig. 3 Conventional TIA-based potentiostat, current-mirror-based potentiostat (top-left) and proposed sensing-current-reused TIA-less current-mirror-less potentiostat (top-right); Circuit implementation of proposed sensing current detector (bottom-left); Timing waveforms of the sensing current detector with SAR logic and BRZ logic (bottom-right).

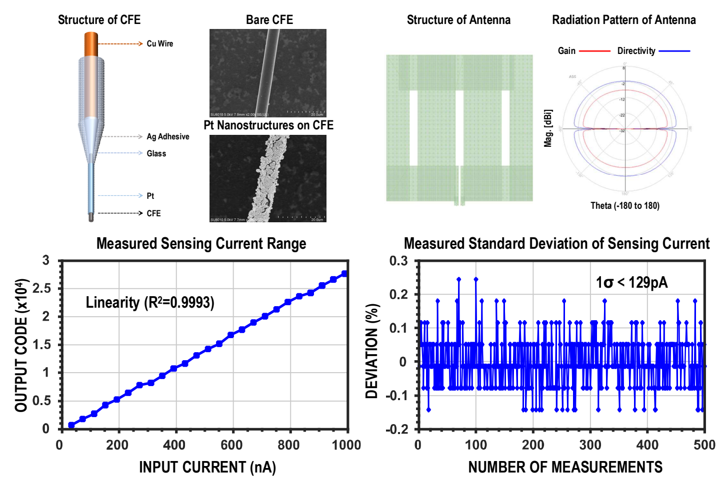

Fig. 4 3D structure and scanning electron microscopy (SEM) images of working electrode (top-left); Structure and simulated radiation pattern of proposed antenna (top-right); Measured sensing current range (bottom-left); Measured standard deviation of sensing current (bottom-right).

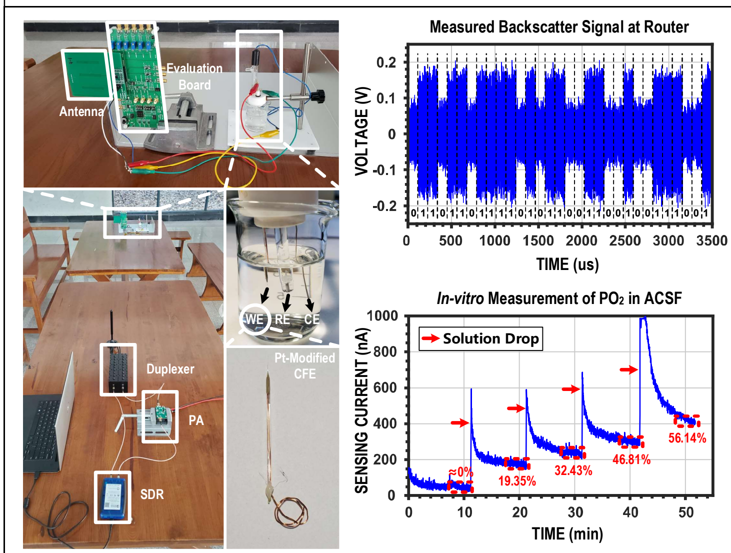

Fig. 5 *In-vitro* measurement setup (left); Measured backscatter signal at router (top-right); *In-vitro* measurement of PO_2 in ACSF (bottom-right).

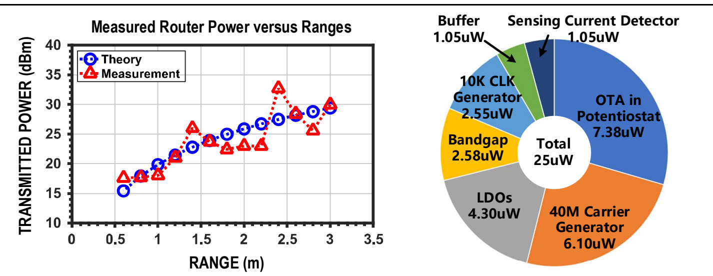

	This Work	ISSCC'20 [1]	JSSC'14 [2]	CICC'20 [3]	TBioCAS'15 [4]	Sensors'18 [5]
Power Supply	Battery-free	Battery-free	Battery	Battery	Battery	Battery
Telemetry	Backscatter	Backscatter	Cable Based	Cable Based	Active RF	Cable Based
Method	Electrochemical	Optical	Electrochemical	Optical	Electrochemical	Electrochemical
Sensor	CFE Based	Film Based	On-Chip	Film Based	Parylene-C Based	On-Chip
Power Consumption	25uW	140uW	42uW	20.6mW	>54mW	1.4mW
Detection Range	0%~56.1%	0.5%~19.8%	1.3%~7.2%	0%~21%	0%~30%	0%~21%
Resolution	0.03%	0.09%@0.5% 0.76%@13.2% 1.1%@19.8%	±0.13%	N/A	N/A	0.06%

Fig. 6 Measured router power versus different wireless-power-transfer ranges (top-left); Power breakdown of COM micro-system (top-right); Performance summary and comparison to state-of-the-art PO_2 sensing systems (bottom).

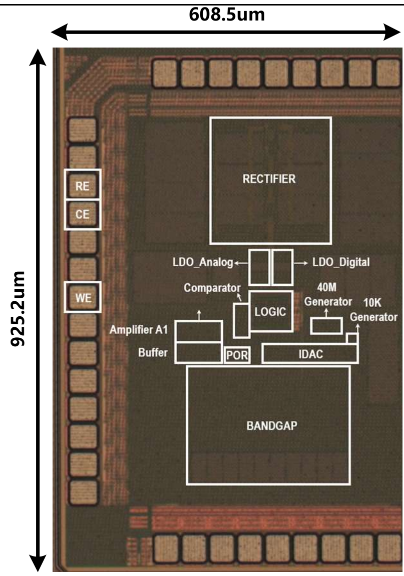

Fig. 7 Die micrograph.

Additional References:

[2] W. P. Chan et al., "A monolithically integrated pressure/oxygen /temperature sensing SoC for multimodality intracranial neuromonitoring," JSSC, 2014

[3] I. Costanzo *et al*., "An integrated readout circuit for a transcutaneous oxygen sensing wearable device," CICC, 2020

[4] P. Mostafalu *et al*., "Wireless flexible smart bandage for continuous monitoring of wound oxygenation," TBioCAS, 2015.

[5] H. Yin *et al*., "CMOS monolithic electrochemical gas sensor microsystem using room temperature ionic liquid," IEEE Sensors Journal, 2018.